# XUV generation at 93 eV for coherent actinic imaging of EUVL mask defects

**Contact** *W.S.Brocklesby@soton.ac.uk*

**W.S. Brocklesby**
*Optoelectronics Research Centre*
*University of Southampton, UK*

**Patrick Anderson**
*Optoelectronics Research Centre*
*University of Southampton, UK*

**Peter Baksh**
*Optoelectronics Research Centre*
*University of Southampton, UK*

**Michal Odstrčil**
*Optoelectronics Research Centre*
*University of Southampton, UK*

**Jeremy G. Frey**
*School of Chemistry*
*University of Southampton, UK*

**Richard T. Chapman**
*Central Laser Facility,*
*STFC Rutherford Appleton Laboratory, UK*

## Introduction

Effective imaging of optical defects in masks for EUV lithography requires the use of the same wavelength as the target design wavelength – so-called 'actinic' imaging. For next-generation lithography at 13.5 nm, microscopy options are limited by the difficulty of obtaining both optics and sources, and scanning microscopy using a synchrotron source is the norm. In this work, we describe development of an alternative 13.5nm imaging system using a source based on high harmonic generation[1]at the Artemis laser facility, and coherent diffractive imaging (CDI) techniques[2]. The requirements on the source are considerable –CDI requires high source coherence, implying narrow bandwidth: in this case, a single harmonic. XUV flux is also critical for CDI measurements, as high signal to noise scattering patterns are needed for accurate phase reconstruction.

This paper will describe testing of several experimental HHG configurations using the Artemis laser, to evaluate the maximum flux available at 13.5 nm. The experimental arrangements necessary for filtering down to a single harmonic will be described, and progress toward 13.5 nm imaging will be reported.

## HHG flux comparisons

Efficiency in HHG is influenced by many factors. High efficiencies require effective phase matching[3], careful management of ionization[4], and use of appropriate wavelengths. The Artemis laser provides a number of options for different HHG schemes which each provide different efficiencies and phasematching possibilities. The initial aim of our work was to provide comparison of several different schemes at a specific wavelength, in this case 13.5 nm, in order to assess which would be the most effective for use in real experiments. Phasematching in all cases was achieved via balance of Gouy shift & atomic phase in a gas jet, as capillary generation is not available at Artemis. Gas species and pump wavelength (and energy) were varied and harmonic output measured.

The different schemes tested were: (1) Ne gas, pumped with pulses at 800 nm, energies up to 5 mJ. (2) Ar or Ne Gas, pumped with a combination of 800nm and its second harmonic at 400nm (3) Ar gas, pumped using the output of the TOPAS OPA system at different wavelengths between 1 – 1.5µm. In principle, the use of longer wavelengths can extend HHG cutoff for a given intensity[5], but the rapid reduction[6] of single atom efficiency with wavelength ($\sim\lambda^{-6}$) must be balanced against extension of cutoff. Isolated reports of very large efficiency increases with simultaneous 800 and 400 nm pumping make that option worth testing.

The direct measurement of total flux for each scheme pumped by a single source is important, as the available pulse energies are limited at each wavelength – as an example, although pumping at 1300 nm may produce higher cutoffs, only 1 mJ is available at Artemis, whereas over 5 mJ are available at 800nm. Similarly, only low energy pulses at 400 nm are available, so comparison of equal energy pulses is not useful.

Very different pump intensities were available at each wavelength, so the focusing geometries were changed between wavelengths to optimize ionization level. For 800nm pumping of Ne, a 1m focal length mirror was used with up to 5 mJ/pulse; for 1300 nm pumping of Ar, a 0.5m focal length mirror was used, with ~1 mJ/pulse. For 800nm + 400 nm pumping, a 0.5m focal length mirror was used for focusing, and the maximum pulse powers used were 2.5mJ at 800nm, and 400 mJ at 400nm. No adjustable delay was available for the 800+400nm experiments, so the 400 nm pulses were generated inside the vacuum chamber, resulting in a walkoff of ~10 fs between the 800 and 400 nm pulses. The 800nm and 400 nm pulses had perpendicular polarizations.

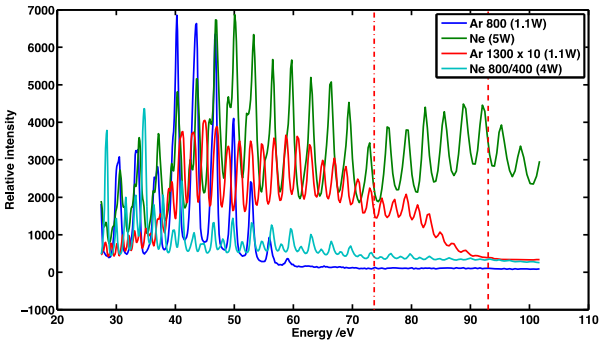


**Figure 1 - comparison of spectra from different generation experiments. The dark blue line is generation in Ar gas using 800nm; green is using Ne with 800 nm pumping. Red is pumping Ar gas at 1300nm and has been multiplied by 10 for visibility, and light blue is combined pumping at 800 & 400 nm. The dotted vertical lines indicate the cutoff of an Al filter (73 eV, used as an aid to wavelength calibration) and the target photon energy (93 eV).**

Figure 1 shows the relative XUV intensities generated at wavelengths between 50 nm and 10 nm (30 eV – 100 eV) for four different pumping schemes. The spectra were measured using a flat-field spectrometer, and the relative intensity scale is correct. In all cases, intensity, gas pressure, and gas jet position were optimized as far as possible.

Pumping of Ar at 800 nm (dark blue) produces little XUV above ~60 eV because of the Cooper minimum[7]. Pumping Ne gas in the same geometry produces a significant extension of the observed XUV radiation out past 100 eV, at which point the

spectrometer sensitivity reduces rapidly. Maximum flux is observed with pulse energies in the range 2 – 4 mJ, and clear nonlinear spectral blueshifts are observable as pulse energy is increased, indicating that phasematching is being disturbed at higher intensities. Pumping using simultaneous 800nm + 400 nm results in enhancement of harmonics at the lower energies – this may be attributable principally to the 400nm component, as the $\lambda^{-6}$ single atom response factor[6] produce an enhancement of a factor of 64. Pumping at 1300 nm produces significantly smaller XUV levels than any of the above techniques – the red graph in Figure 1 is scaled up by a factor of 10 in order to be visible on the plot. The signal reduction factor due to the single atom response would reduce the expected signal level by ~20, and the additional reduction in power because of the lower output of the OPA system exacerbates the reduction in XUV flux.

Overall, the largest flux available at 93 eV across these 4 techniques is by pumping Ne gas with 800 nm pulses – this experimental technique will be used for the rest of the study.

**Absolute flux, and laser filtering**

Collinear HHG always requires separation of the XUV from the pump laser. This is commonly achieved by using thin metal filters that reflect the laser light but transmit in the XUV. At energies below ~73eV, thin (200nm) free-standing Al films are effective, having high reflectivity in the visible and relatively good XUV transmission. At 93 eV, different metals must be used. Several alternatives are possible, notably Nb, Zr, and Mo. In this experiment, we use 200nm Mo films on thin (50 nm) SiN membranes. The membranes support the Mo films and have high transmission around 90 eV (~78%). The overall filter transmission at 93 eV is ~25%. In the visible, the filter transmission was measured to be $\sim 7\times10^{-5}$, higher than the calculated value of $\sim 7\times10^{-6}$ . Thus separation of the XUV and laser is possible, although Mo/SiN filters at 93 eV are less effective than Al filters at 50 eV. Later work suggests that ageing of the filters significantly decreases their initially robust nature.

Based on the measured transmission of the Mo filters, the absolute flux could be measured using the known quantum efficiency of the CCD camera. The flux before the filters was calculated to be $\sim 2\times10^{8}$ photons/sec/harmonic, significantly less than the $6\times10^{11}$ photons/sec/harmonic available[8] around 50 eV with similar laser systems.

In order to produce the necessary coherence for CDI, the XUV beam needs to be filtered to a single harmonic before it is incident on the sample. This is performed using multilayer XUV mirrors with a narrow reflectivity bandwidth. The Mo/Si mirrors used both to filter and focus the XUV beam had reflectivity of 67%, and a reflection bandwidth of 0.5 nm around 13.7 nm. The flux at the sample was $5\times10^{5}$ph/sec. This is enough to perform imaging, but will result in long exposure times.

**CDI imaging geometry**

Imaging using coherent diffraction requires collecting the scattered light from a sample directly onto a detector with no intervening lenses necessary. The scattered intensity distribution is then used as one of two constraints in an optimization problem, which algorithmically determines the phase of the scattered light. Once the phase is known, the original image can be reconstructed by numerical propagation.

The second constraint used in the algorithmic solution can have many forms. Many simple algorithms use the constraint that the sample is known to be on a blank support, effectively oversampling the diffraction pattern. This is useful for simple test objects with no phase variation. More complex extended objects can be imaged using ptychography, where many different scatter patterns are collected, each with slightly different illumination of the object, and the constraint is that overlapping areas of the object in different exposures must have the same structure. Ptychography is more effective in dealing with phase objects, and does not have the inherent degeneracy of solutions common in blank support algorithms such as Hybrid Input/Output CDI (HIO).

Experimentally, the imaging setup is shown in Figure 2. The Mo/SiN filters separate the laserfrom the XUV. The XUV is transmitted, and then focused using the final Mo/Si mirror. The XUV beam passes through a 5 µm aperture, and is incident on the sample. The sample can be moved with high accuracy using a piezo scanning stage. Scattered light from the sample is incident on a cooled XUV CCD camera.

The resolution of the image produced is limited, as in a simple microscope, by the numerical aperture of the collected light. This requires the CCD camera to be mounted very close (in this case, down to ~7 mm) behind the sample itself. The arrangement in Figure 2 allows a numerical aperture for collection of scattered light by the CCD of ~ 0.5, implying an optical resolution of ~15 nm.

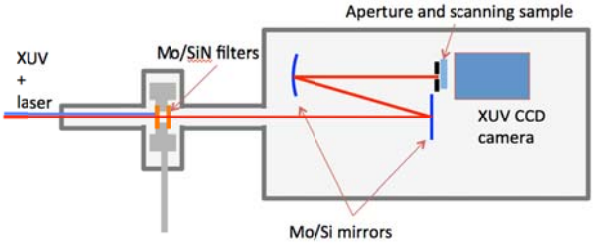


**Figure 2 - Experimental setup for HHG CDI**

The experimental system shown in Figure 2 was set up on the AMO beam line at Artemis. The samples used in this case were small structures written into Au-coated SiN membranes using FIB.

**EUV focal spot size**

Bringing the XUV CCD to the plane of the sample allows a measurement of the focal spot size achieved using the EUV optics. This is important because it will limit the flux through a given pinhole size in a ptychography experiment. The use of a pixellated CCD to measure beam sizes in this way is expected to be accurate to spot sizes down to about half the pixel size, from numerical tests.

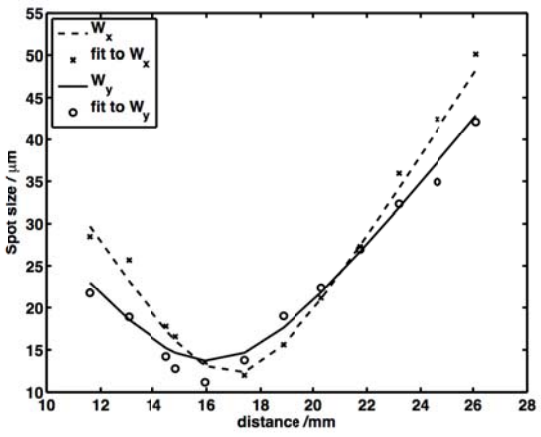


**Figure 3 - measured XUV spot sizes in vertical and horizontal directions**

Figure 3 shows the XUV spot sizes in vertical and horizontal directions, measured using the CCD. The fits to Gaussian propagation are shown. The spot sizes are $W_{0x}$ = 12.1 µm, $W_{0y}$ = 13.7 µm, and the beam propagations factors are $M^2_x$ = 14.4

and $M^2_y$ = 13. The separation of the foci in vertical and horizontal planes of 0.8mm arises from the use of an off-axis spherical mirror for focusing.

The relatively high values of $M^2$ probably arise from aberrations in the XUV mirrors, whose substrates are only polished to flatness appropriate for optical wavelengths. For XUV imaging, the ability to focus to ~10 μm is enough to fill a scanning pinhole, and phase errors will not affect the CDI process. In a ptychography experiment, the probe beam phase is measured as part of the process, allowing confirmation of the propagation measurement.

**Conclusions**

Imaging using CDI in the XUV requires a high flux, focused XUV beam. In this paper we have described initial optimisations of HHG at Artemis for 93 eV photons, suitable for use in investigating defects in lithography phase masks. The flux is measured, and the filtering properties of Mo thin films for separation of the laser and the XUV are characterized. The focusing properties of the EUV mirrors has been evaluated, and spot sizes measured. For imaging purposes, the measured flux is adequate, but higher flux would improve things considerably. The spot sizes measured would be appropriate for ptychography. Before imaging can be performed, measurement of the spatial coherence of the XUV output would be an important further test.

**Acknowledgements**

The authors would like to acknowledge EPSRC and EACEA for PhD studentships, and the Zepler Institute at University of Southampton (Dr Stuart Boden) for fabrication of test samples.

**References**

[1]Corkum, P. Plasma perspective on strong field multiphoton ionization.*Phys. Rev. Lett.***71,** 1994–1997 (1993).

[2]Fienup, J. R. Reconstruction of an object from the modulus of its Fourier transform. *Opt. Lett.***3,** 27–9 (1978).

[3]Balcou, P., Salières, P., L'Huillier, A. &Lewenstein, M. Generalized phase-matching conditions for high harmonics: The role of field-gradient forces. *Phys. Rev. A***55,** 3204–3210 (1997).

[4]Takahashi, E., Kanai, T., Ishikawa, K., Nabekawa, Y. &Midorikawa, K. Coherent Water Window X Ray by Phase-Matched High-Order Harmonic Generation in Neutral Media. *Phys. Rev. Lett.***101,** 253901 (2008).

[5]Popmintchev, T. *et al.* Phase matching of high harmonic generation in the soft and hard X-ray regions of the spectrum. *Proc. Natl. Acad. Sci. U. S. A.***106,** 10516–21 (2009).

[6]Shiner, A. *et al.* Wavelength Scaling of High Harmonic Generation Efficiency.*Phys. Rev. Lett.***103,** 1–4 (2009).

[7]Wahlström, C.-G. *et al.* High-order harmonic generation in rare gases with an intense short-pulse laser. *Phys. Rev. A***48,** 4709–4720 (1993).

[8]Butcher, T. J. *et al.* Bright extreme-ultraviolet high-order-harmonic radiation from optimized pulse compression in short hollow waveguides. *Phys. Rev. A***87,** 043822 (2013).